

RESEARCH

Open Access



Jaw-specific differential kinase activity profiles in human periodontal ligament stem cells under mechanical compression

Christian Niederau^{1*}, Sanne L. Maas², Emiel P. C. van der Vorst^{2,3}, Leon J. Schurgers^{4,5}, Yang Shi⁶, Frank Hölzle⁷, Michael Wolf^{1†} and Rogerio B. Craveiro^{1†}

Abstract

Background Increasing clinical and experimental evidence suggests that the upper and lower jaw exhibit pronounced functional and structural disparities that cannot be explained solely by classical anatomical differences. A central, yet unresolved question is whether periodontal ligament stem cells (PDLSCs) from these distinct regions display site-specific molecular signaling patterns in response to mechanical stress. We propose that PDLSCs derived from maxillary and mandibular regions activate distinct kinase signaling networks upon mechanical stimulation, thereby establishing a jaw-specific mechanobiological fingerprint.

Methods PDLSCs were isolated from seven healthy donor teeth and exposed to a static compressive force of 2 g/cm². Kinase activity was profiled using a high-throughput PamChip® peptide arrays that target both protein tyrosine kinases (PTKs) and serine/threonine kinases (STKs). Downstream pathway enrichment analyses were conducted using the Wikipathways, Gene Ontology (GO), KEGG, and Enriched pathways databases.

Results Mechanical stimulation induced distinct kinase activation signatures depending on jaw origin. Maxillary PDLSCs displayed a predominance of STK activation, while mandibular cells showed a relative reduction in PTK signaling. Only two PTKs and four STKs were consistently regulated across both regions, supporting the presence of a region-specific mechanotransduction profile.

Conclusion These findings support our hypothesis that localized differences in kinase signaling may constitute a molecular basis for the clinically observed jaw-specific phenomena, such as heterogeneous orthodontic tooth movement and alveolar bone remodeling. Jaw-dependent mechanotransduction pathways can therefore be considered key determinants of periodontal biology and may provide a basis for follow-up studies aimed at enabling the development of personalized orthodontic and regenerative strategies.

Keywords Upper jaw, Lower jaw, Kinase activity, Kinomics, PamGene, Human PDL, PDLSC, hPdlF, Tooth movement, Maxilla, Mandible

[†]Michael Wolf and Rogerio B. Craveiro contributed equally to this work.

*Correspondence:
Christian Niederau
cniederau@ukaachen.de

Full list of author information is available at the end of the article



© The Author(s) 2025. **Open Access** This article is licensed under a Creative Commons Attribution 4.0 International License, which permits use, sharing, adaptation, distribution and reproduction in any medium or format, as long as you give appropriate credit to the original author(s) and the source, provide a link to the Creative Commons licence, and indicate if changes were made. The images or other third party material in this article are included in the article's Creative Commons licence, unless indicated otherwise in a credit line to the material. If material is not included in the article's Creative Commons licence and your intended use is not permitted by statutory regulation or exceeds the permitted use, you will need to obtain permission directly from the copyright holder. To view a copy of this licence, visit <http://creativecommons.org/licenses/by/4.0/>.

Introduction

The periodontium, a multifunctional tissue complex, serves as the principal anchoring system for teeth within the alveolar bone, integrating mechanical support with biological responsiveness. It consists of mineralized and soft tissues, including the alveolar bone, periodontal ligament (PDL), cementum, and gingiva, which work in concert to maintain stability and respond to mechanical forces [1, 2]. The most common cells within the PDL are periodontal ligament stem cells (PDLSC). As a central component of the periodontal apparatus, they are key regulators of the microenvironment and essential for tooth attachment and nutrition, as well as performing functions of proprioception, buffering of acting forces, enabling periodontal remodelling, and transmission of mechanical signals. The extracellular matrix produced by PDLSCs constitutes the structural framework surrounding the tooth root and plays a pivotal role in maintaining tissue homeostasis within the periodontium [3–6].

When orthodontic forces are applied, the tooth moves within its bony socket, resulting in the formation of zones of tension and compression [7, 8]. Mechanical stress applied to the PDL initiates a cascade of biological processes that enable controlled tooth movement (OTM) through the bone. Here, the PDL plays a central role by transmitting mechanical forces through collagen fibers, particularly Sharpey's fibers, while maintaining flexibility [9, 10].

Intercellular crosstalk within the periodontal microenvironment is essential in orchestrating localized tissue remodeling and preserving the functional integrity of the periodontium [1]. Mechanical stress-induced remodeling of soft and hard periodontal tissue involves a coordinated interplay among osteoclasts, osteoblasts, fibroblasts, vascular networks, and immune cell populations within the PDL [8, 9].

In compression zones, osteoclasts, which reach the local area from periodontal blood vessels [11, 12], can resorb the alveolar bone to enable tooth movement in the direction of the applied force, while in tension zones, osteoblasts deposit new bone to stabilize the tooth. This dynamic remodelling is regulated by multiple signalling pathways that control the release of RANKL/OPG and cytokines amongst others, which are essential for bone remodelling processes by increased osteoclast activation [13].

These processes appear to differ between the upper (maxilla) and lower jaws (mandible), which have different anatomical and physiological features that impact wound healing, disease prevalence, and the speed of orthodontic tooth movement. For example, orthodontic tooth movement is significantly faster in the maxilla than in the mandible [14–16]. This difference is primarily due to the structural composition of the bones. The upper jaw

consists mainly of trabecular bone, which is less dense and more porous, allowing for faster bone remodelling during OTM. In contrast, the mandible contains a higher proportion of cortical bone, which is denser and more resistant to resorption and deposition processes [17]. This structural disparity slows down the rate at which teeth can move in the mandible compared to the maxilla [18, 19]. Additionally, vascularization plays a significant role in these upper and lower jaw-specific differences. The maxilla's richer blood supply enhances cellular activity and may accelerate bone turnover, facilitating faster tooth displacement. Contrarily, the mandible's relatively lower vascularization may contribute to slower remodeling [20, 21]. These findings underscore the necessity of incorporating jaw-specific biological characteristics into orthodontic treatment to enhance therapeutic precision and predictability.

Additionally, all these jaw-specific characteristics have been observed in functional clinical practice. A more detailed investigation into the molecular factors that promote jaw-specific clinical characteristics is needed. Only a few pioneering studies have investigated differences in cell signaling between human periodontal ligament stem cells from the upper and lower jaw under mechanical stimulation [22–24]. Most previous studies on periodontal remodelling and orthodontic tooth movement have not taken into account the jaw-specific differences between the upper and lower jaw. However, there are initial indications that the cytokine content in the gingival crevicular fluid in the upper jaw may differ from that in the lower jaw [23].

In a previous study without mechanical stimulation, we demonstrated that PDLSCs from the upper region exhibit significantly higher proliferation and differentiation potential than those from the lower region [6]. Further, under physiological conditions the kinase activity in the lower jaw appeared higher than in the upper jaw [25]. Based on these findings, we hypothesised that kinomics, which measures kinase activity, should reflect the key inherent features of PDLSC cell-specific regulatory networks from the maxilla and mandible that determine the regenerative potential of PDLSC and thus explain differences in clinical observations.

We propose that periodontal ligament stem cells derived from the maxilla and mandible activate distinct kinase signaling networks in response to mechanical stimulation, thereby establishing a region-specific mechanobiological fingerprint. To elucidate these signatures, we used PamChip® peptide array-based assays to systematically profile kinase activity and downstream signaling pathways in human PDLSCs isolated from the maxilla and mandible of the same donor under standardized compressive force. These assays targeted phosphotyrosine kinases (PTKs) and phospho-serine/

threonine kinases (STKs). This experimental strategy enables region-specific kinase activity signatures to be discriminated in genetically matched cells, minimizing donor variability and allowing subtle, jaw-dependent differences in mechanotransduction to be detected. By delineating these molecular signatures, we aim to identify the key regulatory kinases involved in mechanically induced periodontal remodeling, as well as the associated signaling pathways. These insights are expected to provide a conceptual framework for future pathway-centric research into the molecular dynamics of PDLSCs and could ultimately inform precision approaches in orthodontic and regenerative therapies, which are tailored to specific biological contexts.

Materials and methods

Study design

Human periodontal ligament stem cells were obtained from seven patients (4 male, 3 female, aged 18–31 years). Detailed information about the donors and the specific teeth is shown in Table 1. The collection and use of periodontal cells derived from discarded patient biomaterial was authorized by the Ethics Committee of the University of Aachen, Germany (approval number EK 374/19), and all procedures adhered to relevant ethical guidelines and regulations. Informed consent was secured from all participants or their legal representatives. Primary human PDLSCs were isolated and analyzed for the expression of specific stem cell markers as well as their differentiation into adipocytes, chondrocytes, and osteoblasts, as outlined in previous studies [6, 25]. Subsequently, human PDLSCs were cultured in six-well plates until reaching 90–100% confluence. After a 24-hour incubation period, a static compressive force of 2 g/cm² (0.02 N/cm²) was applied for 24 h to the monolayer using sterile round

glass cylinders (34 mm diameter; 18 g), following the protocol established by Kanzaki et al. [26]

To obtain sufficient material, cells from two wells of a 6-well plate were lysed and combined into a single pooled sample for further processing. Total protein was quantified before loading the lysates onto corresponding PamChips® for PTK (tyrosine kinase) and STK (serine/threonine kinase) analysis. This leads to 7 biological replicates from different donors analyzed in independent arrays on the PamChips®. Kinase activity profiles of PDLSCs derived from the upper and lower jaw of the same individual were then comparatively analyzed under conditions with and without applied compressive force (Fig. 1). Peptide phosphorylation patterns are represented in volcano plots, and kinase activity is visualized in heatmaps. Pathway analysis was performed with a primary focus on signaling pathways related to inflammation, hypoxia, vascularization, immune modulation, bone remodeling, and wound healing.

Samples and cell culture

Human PDLSCs were obtained from the periodontal connective tissue of the middle root section of decay-free human teeth, freshly extracted for medical purposes at the dental clinic of the University Hospital RWTH Aachen. The isolation procedure followed previously published protocols [5, 24]. Isolated PDLSCs have previously been characterized based on criteria established by the International Society for Cellular Therapy, including the evaluation of specific surface markers and their ability to differentiate into adipocytes, chondrocytes, and osteoblasts in vitro [5, 24, 25].

Tyrosine and serine/threonine kinase activity profilig

The PamChip® microarray system on the PamStation®12 platform (PamGene International, s'Hertogenbosch, The Netherlands) was employed to analyze PTK and STK activity profiles. The PTK-PamChip® arrays contain 196 unique phospho-sites, while the STK-PamChip® arrays include 144 unique phospho-sites, representing peptide sequences derived from PTK and STK substrates, respectively. Phosphorylation of peptides was detected via fluorescence resulting from the binding of a FITC-conjugated antibody, which specifically recognizes the phosphorylated phospho-sites (Fig. 1).

Human PDLSCs from the maxilla and mandible were cultured in six-well plates at passage two until reaching approximately 80% confluence. Cells were washed with ice-cold PBS and lysed on ice for 15 min using M-PER Mammalian Extraction Buffer (Thermo Fisher Scientific, Waltham, USA) supplemented with Halt Phosphatase Inhibitor and EDTA-free Halt Protease Inhibitor Cocktail (1:100 each; Thermo Scientific). Lysates were centrifuged

Table 1 Detailed information about donors and specific teeth. If two teeth are specified for one jaw, this means that the cells of both teeth have been pooled

Donor Patient	Age (yrs)	Sex	Tooth location (FDI)
1	18	female	18, 28 38, 48
2	20	female	18, 28 48
3	31	female	28 38
4	19	male	28 38
5	19	male	28 38, 48
6	18	male	18, 28 38
7	22	male	18 48

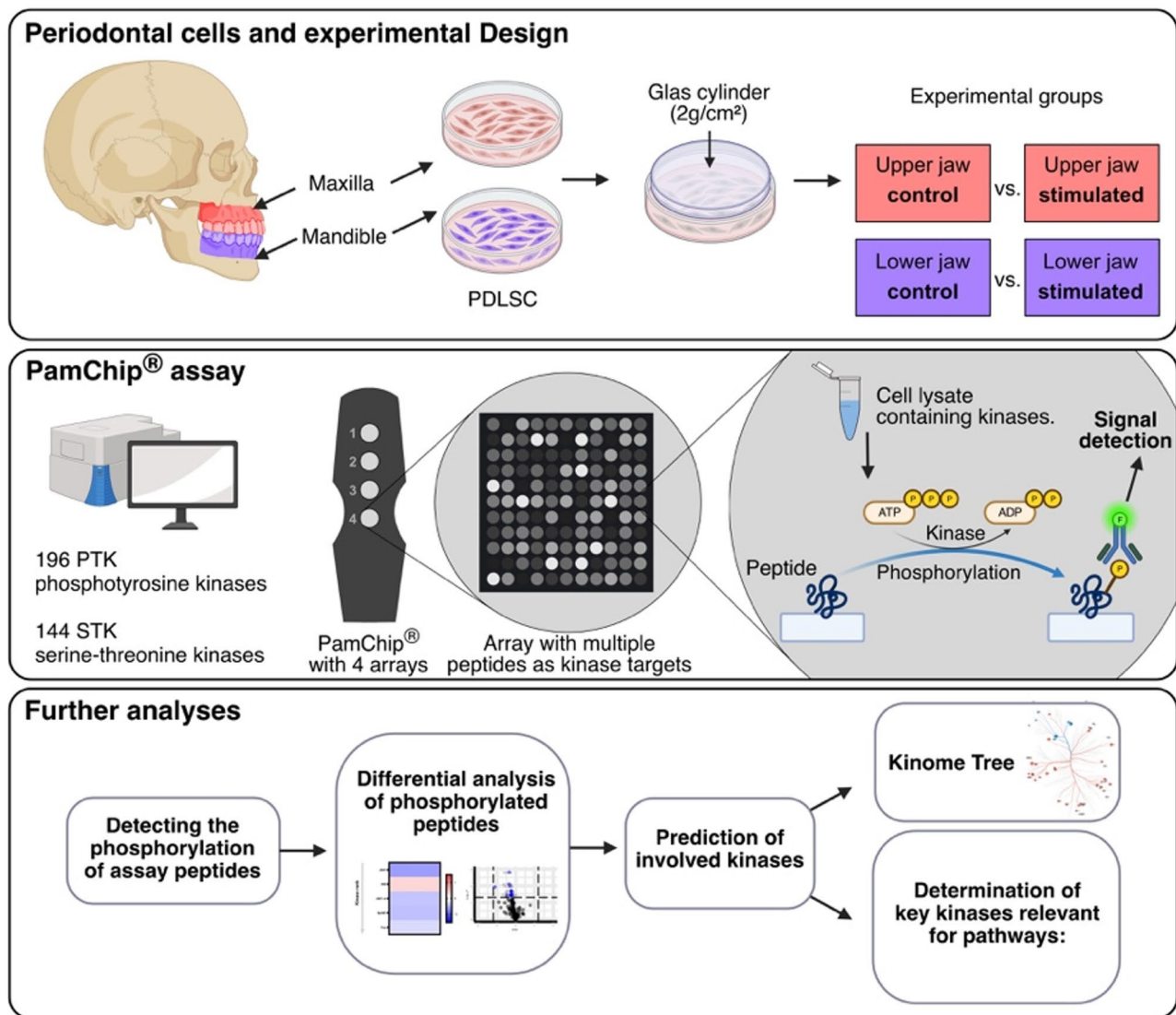


Fig. 1 Schematic diagram of the study design. Molars from healthy donors were extracted from the upper and lower jaws of the same donors. The periodontal ligament (PDL) was removed from the tooth and the human periodontal ligament stem cells (hPDLSCs) were isolated. After an incubation period of 24 h, a static force of 2 g/cm² was applied to the monolayer using sterile round glass cylinders. The lysed cells were analysed using PamChips[®] for PTK (tyrosine kinase) and STK (serine/threonine kinase) kinomics technology and kinomics analysis was performed

at 12,000 g for 15 min at 4 °C in a pre-cooled centrifuge, and the supernatant was collected. Protein concentrations were determined using the Pierce[™] Coomassie Plus (Bradford) Assay (Thermo Fisher Scientific, Waltham, USA), according to the manufacturer's protocol.

For the PTK assay, 10 µg of protein per array was used following the standard PamGene protocol with provided reagents. The PTK Basic Mix was prepared by combining freshly frozen lysate with 4 µL of 10× protein PTK reaction buffer (PK), 0.4 µL of 100× bovine serum albumin (BSA), 0.4 µL of 1 M dithiothreitol (DTT), 4 µL of 10× PTK additive, 4 µL of 4 mM ATP, and 0.6 µL of monoclonal FITC-conjugated anti-phosphotyrosine detection antibody (clone PY20). The final volume was adjusted to

40 µL with distilled water. Prior to loading the PTK Basic Mix onto the arrays, a blocking step was performed using 30 µL of 2% BSA followed by washing with PTK solution for preprocessing. Subsequently, 40 µL of PTK Basic Mix was applied to each array, and microarray testing was conducted over 94 cycles. Images were captured using a CCD camera on the PamStation[®]12 during kinetic read cycles 32–93 at exposure times of 10, 50, and 200 ms, as well as during end-level read cycles at exposure times of 10, 20, 50, 100, and 200 ms.

For the STK assay, each array was loaded with 2.0 µg of protein and 400 µM ATP along with an STK Basic Mix, consisting of 1× protein PTK reaction buffer (PK), 1× bovine serum albumin (BSA) and 1× STK antibody

mix. Prior to loading the STK Basic Mix onto the arrays, a blocking step was performed using 30 μL of 2% BSA followed by washing with PTK solution for preprocessing. Subsequently, 40 μL of STK Basic Mix was applied to each array. A FITC-conjugated antibody was applied to visualize phosphorylation after one hour of incubation at 30 °C. During this incubation, samples were pumped back and forth through the porous material to enhance binding kinetics and reduce assay duration. Imaging was performed using an LED-based imaging device, and spot intensities were measured at each time point after adjusting for local background.

Data analysis was conducted using BioNavigator software version 6.3 (PamGene International). No blinding was performed in our study because all analyses were conducted using the standardized and fully automated PamChip® assay platform, which relies on predefined, objective read-out parameters. Since proper balancing of the chips is required to ensure this standardisation, the operator must be aware of the conditions. The data acquisition and quantification are software-based and independent of operator interpretation, thereby minimizing the risk of observer bias.

Prediction of upstream kinases

For both PTK and STK assay, Upstream Kinase Analysis (UKA), a functional scoring method (PamGene) was used to rank kinases based on combined specificity scores (based on peptides linked to a kinase, derived from 6 databases) and sensitivity scores (based on treatment-control differences). Data is represented as mean kinase statistics (adjusted p -value < 0.05) and node size median final score (>1.2). The specificity score reflects the association of a kinase with its corresponding peptides, as curated from six databases, while the sensitivity score captures the magnitude of phosphorylation changes between treatment and control conditions. The resulting median final score integrates these two components, providing a measure of the kinase's overall activity. A median final score greater than 1.2 indicates a consistent and biologically relevant regulation of kinase activity across multiple peptides, distinguishing true activation events from background variation. Kinases meeting this threshold (adjusted p -value < 0.05) were considered significantly regulated and are represented in the network visualization by increased node sizes. For detailed information about the algorithms used, please refer to the PamChip® documentation. The distribution of the phosphorylated peptides is shown in the volcano plots created with the R package EnhancedVolcano [27]. Blue dots depict peptides with an adjusted P value < 0.05. The active kinases are represented in a heatmap; the color scale indicates mean kinase statistic, and the kinase ranking is based on the median final score. Additionally, the kinases can be

depicted in a coral tree to visualize the kinase families; here, node/branch colors represent mean kinase statistics, and node sizes represent the median final scores.

Pathway analysis and differential analysis

Over-representation analysis (ORA) of the Kyoto Encyclopedia of Genes and Genomes (KEGG) database for the kinases with significant differences (median final scores >1.2 and adjusted p -value < 0.05) was performed using the R packages clusterProfiler [28] Data was visualized with the R package ggplot2 [29].

Pathway enrichment analysis was performed on the differentially expressed kinases. The R package disease ontology semantic and enrichment analysis (DOSE) [30] was utilized to analyze the biological complexities in which these kinases correlate with multiple annotation categories, which was visualized with the R package ggplot2 [29] in a dotplot and/or in a network plot with the help of the R package Reactome Pathway Analysis (ReactomePA) [31].

Sample size calculation

The required sample size for the cell culture experiments was estimated a priori using a power analysis based on previously published results for the phosphorylation of pP38 [5]. The calculation was performed using GPower 3.1 [32], assuming an expected effect size of 2.453, a significance level (α) of 0.05, and a statistical power ($1-\beta$) of 0.95. Based on these parameters, a minimum of 6 independent samples per group was required to detect a statistically significant difference.

To ensure reproducibility and account for potential data loss or experimental variation, we included 7 independent biological replicates per condition in all experiments.

Statistical analysis

Overall, the kinase data is represented as significantly different when the median final scores are higher than 1.2 and the adjusted p -value is lower than 0.05. All statistical analysis was conducted using R and are described in greater detail in the sections "Prediction of Upstream Kinases" and "Pathway Analysis and Differential Analysis" above.

Results

The data presented on PDLSCs are based on self-isolated human PDLSCs from the upper and lower jaws of different donors and have already been characterized in our previous studies. The PDLSCs also showed similar characteristics in the evaluation of stem cell character [5, 6, 24, 25] as described in the basic protocols defined by the International Society for Cellular Therapy for

mesenchymal stem/stromal cells and for periodontal ligament stem cells [33].

To determine protein kinase activity profiles of PDLSCs from the upper and lower jaw without stimulation and under compressive force, we applied PamChip® technology (PamGene, Hertogenbosch, Netherlands) to analyze kinase activity in PDLSCs from seven donors.

Phosphorylation of PTK-peptides in the lower jaw was more widely regulated than STK under compressive forces
Protein tyrosine kinase (PTK) analysis revealed that 137 PTK-specific peptides in the upper and lower jaw were phosphorylated. Of these, 11.67% (16/137) were significantly down-regulated in the lower jaw, whereas in the upper jaw 0.45% (3/137) were regulated (2 up-regulated and 1 down-regulated). STK-specific peptides showed that 87 peptides were phosphorylated in both jaws. Only up-regulated phosphorylation of peptides was observed in both jaws: 0.034% (3/87) in the lower jaw and 0.057% (5/87) in the upper jaw. Interestingly, only one peptide (RBL2-655-667) shows a significant change in phosphorylation in both the lower and upper jaw. All other significant differences are specific to each jaw. A detailed list of all peptides whose phosphorylation status changed significantly in response to compressive force stimulation in the upper and lower jaw can be found in Table 2 and Figs. 3A and 4A.

As a next step, Upstream Kinase Analysis was performed to identify the kinases that are potentially responsible for the phosphorylation patterns observed on PamChip® peptides. The identified kinases were scored according to their statistical relevance to the corresponding peptide sets.

Following the prediction, an analysis of the upper jaw using PTK revealed that 73 kinases were active. Of these, 93.1% (68/73) were not significantly differently regulated. IRR (Insulin Receptor kinase) is the only up-regulated kinase in PDLSCs of the upper jaw under compressive force, compared to control, and accounted for 1.4% (1/73) of all kinases. In comparison, 5.5% (4/73, JAK3, JAK1b, ErhB3, and Fyn) of the kinases were down-regulated in these samples. PTKs from the lower jaw were found to be more down-regulated in PDLSCs after subjecting them to compressive force compared to control (57.5%; 42/73).

Predicted STKs from the upper jaw showed that 92 kinases were active in PDLSCs exposed to force. In this case, 36.9% (34/92) were up-regulated, while 63% (58/92) were not significantly differently regulated. STKs from the lower jaw were less differently active compared to control: 10% (10/92) were up-regulated, while 90% (82/92) were not differently regulated between the two conditions. (Fig. 2). Table 3 provides a detailed listing of the top 10 regulated PTKs and STKs in PDLSCs under

compressive force relative to control from lower and upper jaw.

STK activity was strongly up-regulated and PTK activity showed slight differences under compressive force in the upper jaw

The activity of STKs in the upper jaw was significantly up-regulated, while on the other hand, only a few PTKs were down-regulated. The kinases that had a significantly different activity in the upper jaw under compressive force compared to unstimulated control were visualized on the Coral kinome tree plot (Fig. 3C). The mean kinase statistics values (adjusted p-value, shown in Table 3), encoded in branch color, indicate the overall change of the peptide set that represents the kinase, with an adjusted p-value of <0.05 indicating kinase upregulation of PDLSC from compressive force compared to control (Fig. 3B and C). Specific enhancement of STK was observed in a broad spectrum of kinase families of the human kinome. The CMGC kinase family, named after the initials of its main kinase families (CDKs, MAPKs, GSKs, and CLKs), includes key kinases: the MAPK growth- and stress-response kinases, the cell cycle (cyclin dependent kinases - CKD), and kinases involved in splicing and metabolic control. This kinase family regulates the progression through the different phases of the cell cycle in association with their activating partners, cyclins. The calcium and calmodulin-dependent protein kinase family (CAMK) is involved in the phosphorylation of transcription factors and, therefore, in the regulation of expression of responding genes. The casein kinase family (CK1) is also involved in cell cycle, transcription and translation, the structure of the cytoskeleton, cell-cell adhesion and receptor-coupled signal transduction and protein kinase A, G, and C family (AGC) (Fig. 3C).

PTK activity was strongly down-regulated under compressive force in the lower jaw

In contrast to the upper jaw, the lower jaw exhibited a strong downregulation of the tyrosine kinase (TK) family (Fig. 4). This kinase family plays a crucial role in transmitting extracellular signals into the cell: more than half of all TKs are receptor tyrosine kinases (RTKs) located at the cell surface. At the same time, many of the remaining members function near the cell membrane. Additionally, the lower jaw showed upregulation of STK activity, specifically involving kinases from the CMGC and AGC families, as well as AMPK α from the CAMK family.

Selection of signalling pathways revealed different regulatory network analysis in the maxilla and mandible under compressive forces

In order to gain mechanistic insights into the regulatory pathways underlying the differential development of the

Table 2 A strong difference between the PTK and STK kinase activity profiles was observed when comparing the upper and lower jaws under compressive forces

Upper jaw									
PTK peptides					STK peptides				
ID	Uniprot Accession	Sequence	delta_Force	TTest_p_Force	ID	Uniprot Accession	Sequence	delta_Force	TTest_p_Force
VGFR3_1061_1073	P35916	DIYKDP-DYVRKGS	0,535	0,014	RBL2_655_667	Q08999	GLGRS-ITSPTTLY	0,500	0,003
DYR1A_212_224	Q13627	KHDTEM-KYYIVHL	0,981	0,032	RB_803_815	P06400	NIYISPLK-SPYKI	0,204	0,019
DCX_67_79	O43602	GIVYAVSS-DRFRS	-0,172	0,035	KCNA2_442_454	P16389	PDLKKSRSASTIS	0,599	0,041
					FRAP_2443_2455	P42345	RTRTD-SYS-AGQSV	0,614	0,042
					KCNA1_438_450	Q09470	DSDL-SRRSSST-MS	0,724	0,045
Lower jaw									
PTK peptides					STK peptides				
ID	Uniprot Accession	Sequence	delta_Force	TTest_p_Force	ID	Uniprot Accession	Sequence	delta_Force	TTest_p_Force
CDK4_11_23	P11802	EIGVGAYGT-VYKA	-0,352	0,002	CDK7_163_175	P50613	GSPNRAY-THQVVT	0,313	0,005
EFS_246_258	O43281	GGTDEGIYD-VPLL	-0,355	0,008	RBL2_655_667	Q08999	GLGRS-ITSPTTLY	0,294	0,024
YES_420_432	P07947	LIEDNEYTAR-QGA	-0,306	0,011	NEK3_158_170	P51956	FAC-TYVGT-PYYVP	0,299	0,045
EGFR_1103_1115	P00533	GSVQNPVYH-NQPL	-1,110	0,012					
CDK2_8_20	P24941	EKIGEGTYGV-VYK	-0,244	0,020					
HAVR2_257_267	Q8TDQ0	GIRSEENIYTI	-0,255	0,020					
EPHA2_765_777	P29317	EDDPEATYTT-SGG	-0,245	0,022					
PAXI_111_123	P49023	VGEEHVYS-FPNK	-0,238	0,025					
KIT_930_942_C942S	P10721	ESTNHIYSN-LANS	-0,203	0,034					
NTRK2_696_708	Q16620	GMSRDVYST-DYYR	-0,260	0,035					
MK12_180_189_M182B	P53778	SEBTGYVWTR	-0,265	0,035					
PECA1_708_718	P16284	DTETVYSEVRK	-0,198	0,036					
PGFRB_768_780	P09619	SSNYMAPY-DNYVP	-0,481	0,036					
ENOG_37_49	P09104	SGASTGI-YEALEL	-0,283	0,036					
CD79A_181_193	P11912	EYEDENLY-EGLNL	-0,270	0,038					
PTN6_531_541	P29350	GQESEYGNITY	-0,212	0,045					

Comparison of significantly different PTK- and STK-specific peptides. Bold text indicates an upregulation PTK by compressive force, regular text indicates a downregulation of peptide phosphorylation. A p-value < 0.05 was considered statistically significant

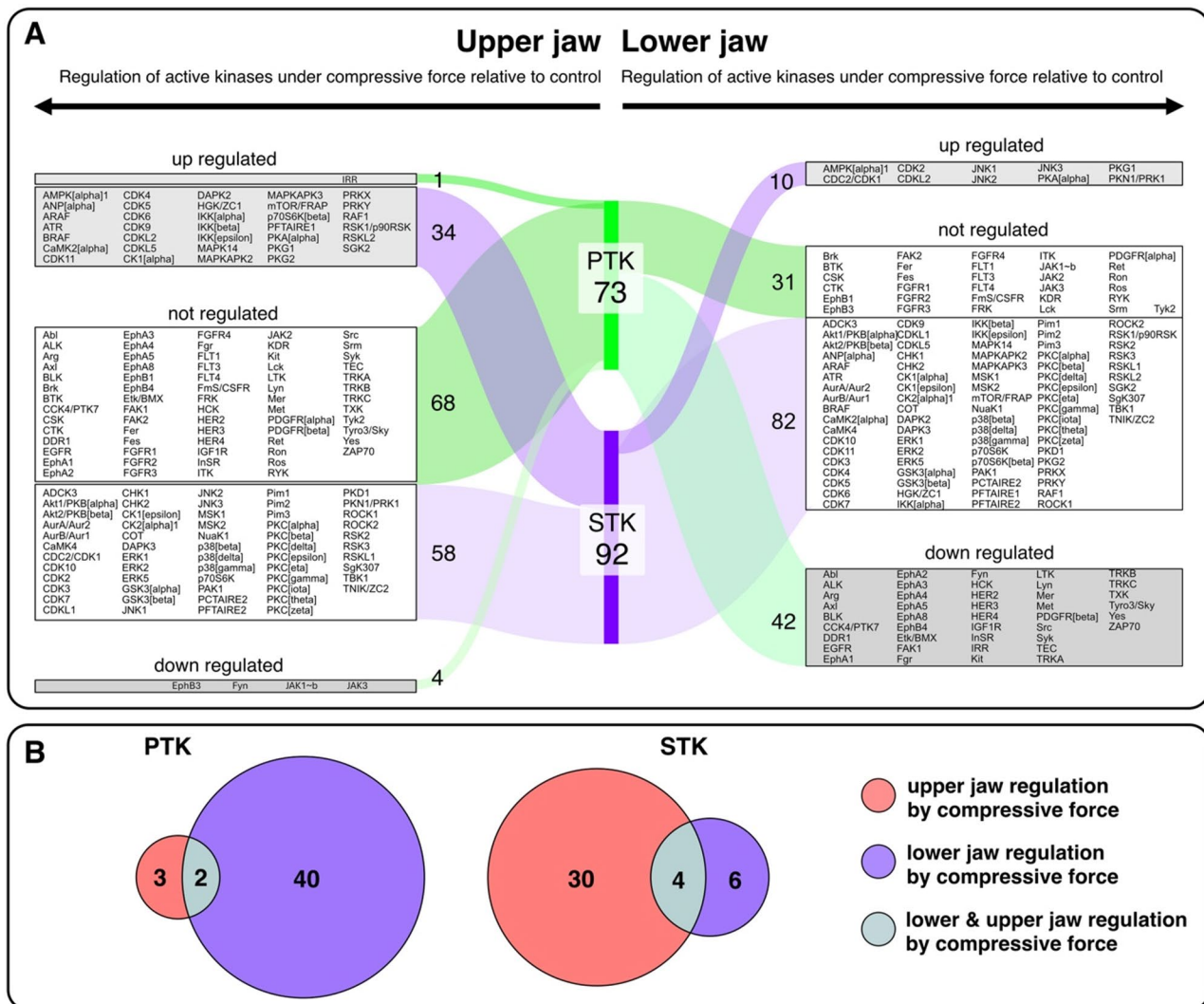


Fig. 2 Regulation of active kinases. **A** Sankey diagram illustrating differential kinase activity profiles in periodontal ligament stem cells from the upper and lower jaw under compressive force compared to control. A pronounced difference in kinase activity was observed between PTK (tyrosine kinases) and STK (serine/threonine kinases) when comparing PDLSC derived from the maxilla (upper jaw) and mandible (lower jaw) under mechanical compression. The diagram visualizes shifts in phosphorylation patterns, highlighting distinct jaw-specific signaling responses. Not active kinases are not shown (123 PTK and 52 STK) **B** Comparison of regulated kinases between upper and lower jaw. (The data shown are derived from experiments performed with PDLSCs obtained from seven different donors)

maxilla and mandible under compressive forces, we performed ORA to the most important processes in the periodontal remodelling of periodontal ligament cells under compressive forces. For this purpose, four data bases were included, namely the Gene Ontology (GO), Kyoto Encyclopedia of Genes and Genomes (KEGG), Wikipathways and Enriched pathways. Table 4 shows the selected signalling pathways that potentially contribute to key biological processes in the remodelling of the periodontium under compressive forces. A visualisation of the numerical ratios of jointly and jaw-specific regulated signalling pathways is shown in Fig. 5. Overall, a large proportion of the signalling pathways are only regulated in one jaw

(Fig. 5). Detailed information about regulated pathways is shown in additional files 2–5.

Visualization of the a number of jaw-specific signalling pathways that are regulated by mechanical stimulation quantitative relationships between the signaling pathways regulated by mechanical stimulation in the upper and lower jaw, based on various databases: enrichment pathways, Gene Ontology (GO), Kyoto Encyclopedia of Genes and Genomes (KEGG), Wikipathways and Enriched Pathways. (The data shown are derived from experiments performed with PDLSCs obtained from seven different donors.)

Table 3 Top 10 PTK and STK predicted upstream kinases from lower and upper jaw

Upper jaw							
PTK				STK			
Kinase Name	Kinase Uniprot ID	Mean Kinase Statistic	Median Final Score	Kinase Name	Kinase Uniprot ID	Mean Kinase Statistic	Median Final Score
JAK3	P52333	-0.571	2.996	CDKL2	Q92772	0.646	3.333
IRR	P14616	0.310	1.609	ANP alpha	P16066	0.487	2.585
JAK1 beta	P23458	-0.351	1.552	CDK11	Q9BWU1	0.576	2.465
EphB3	P54753	-0.373	1.345	HGK/ZC1	O95819	0.647	2.403
Fyn	P06241	-0.221	1.266	CDK4	P11802	0.542	2.303
				CDK6	Q00534	0.537	2.303
				MAPKAPK3	Q16644	0.442	2.179
				SGK2	Q9HBY8	0.506	2.049
				CDKL5	O76039	0.438	1.917
				ATR	Q13535	0.530	1.892
Lower jaw							
PTK				STK			
Kinase Name	Kinase Uniprot ID	Mean Kinase Statistic	Median Final Score	Kinase Name	Kinase Uniprot ID	Mean Kinase Statistic	Median Final Score
Lyn	P07948	-0.826	3.690	JNK2	P45984	0.297	1.893
SyK	P43405	-0.646	3.665	PKG1	Q13976	0.251	1.610
ZAP70	P43403	-0.662	3.627	CDKL2	Q92772	0.331	1.563
EphA5	P54756	-1.393	2.887	CDK2	P24941	0.277	1.494
TRKB	Q16620	-0.686	2.788	AMPK alpha	Q13131	0.301	1.419
Abl	P00519	-0.637	2.695	PKN1/PRK1	Q16512	0.303	1.390
Arg	P42684	-0.647	2.600	PKA alpha	P17612	0.232	1.354
EphA8	P29322	-1.112	2.473	JNK3	P53779	0.256	1.236
Fgr	P09769	-0.978	2.414	JNK1	P45983	0.252	1.215
Src	P12931	-0.678	2.370	CDC2/CDK1	P06493	0.241	1.213

Bold text indicates an upregulation by compressive force, regular text indicates a downregulation

Discussion

Clinical observations suggest that the bone remodeling capacity, with focus on tooth movement rate in the alveolar bone, tends to be faster and more effective in the maxilla compared to the mandible [14–16]. In both upper and lower jaws, PDLSCs are the predominant cell type within the periodontal ligament playing a crucial role in maintaining the periodontal apparatus. These cells contribute to tooth anchorage and nutrition, and are involved in proprioception, force buffering, periodontal remodeling, and the transmission of mechanical stimuli [34]. These properties identify PDLSCs as key regulators of periodontal remodelling [9]. According to current research, the in vitro models available to date provide a comprehensive picture of the processes of periodontal remodelling under mechanical stimulation and its potential modulation possibilities [5, 35–38]. However, none of these studies have distinguished between the maxilla and mandible, meaning that potential jaw-specific intracellular signalling pathways have remained undiscovered,

even though clinical observations suggest such differences exist.

These are evident, for example, in increased interleukin levels in the gingival crevicular fluid of the upper jaw, which was obtained from the periodontal ligament surrounding the tooth [23].

In this study, we present a novel strategy to investigate jaw-specific metabolic differences in mechanical response and remodeling capacity by analyzing variations in intracellular kinase activity in PDLSCs. This methodology allowed us to discriminate region-specific responses in cells from healthy donors during mechanical stimulation.

By specifically examining PDLSCs from the upper and lower jaw, we were able to show for the first time that the kinase profile after mechanical stimulation differs significantly between the maxilla and mandible. In general, PTKs were mainly downregulated in both jaws while STKs were upregulated. However, the respective number of regulated kinases is striking. While only a few PTKs

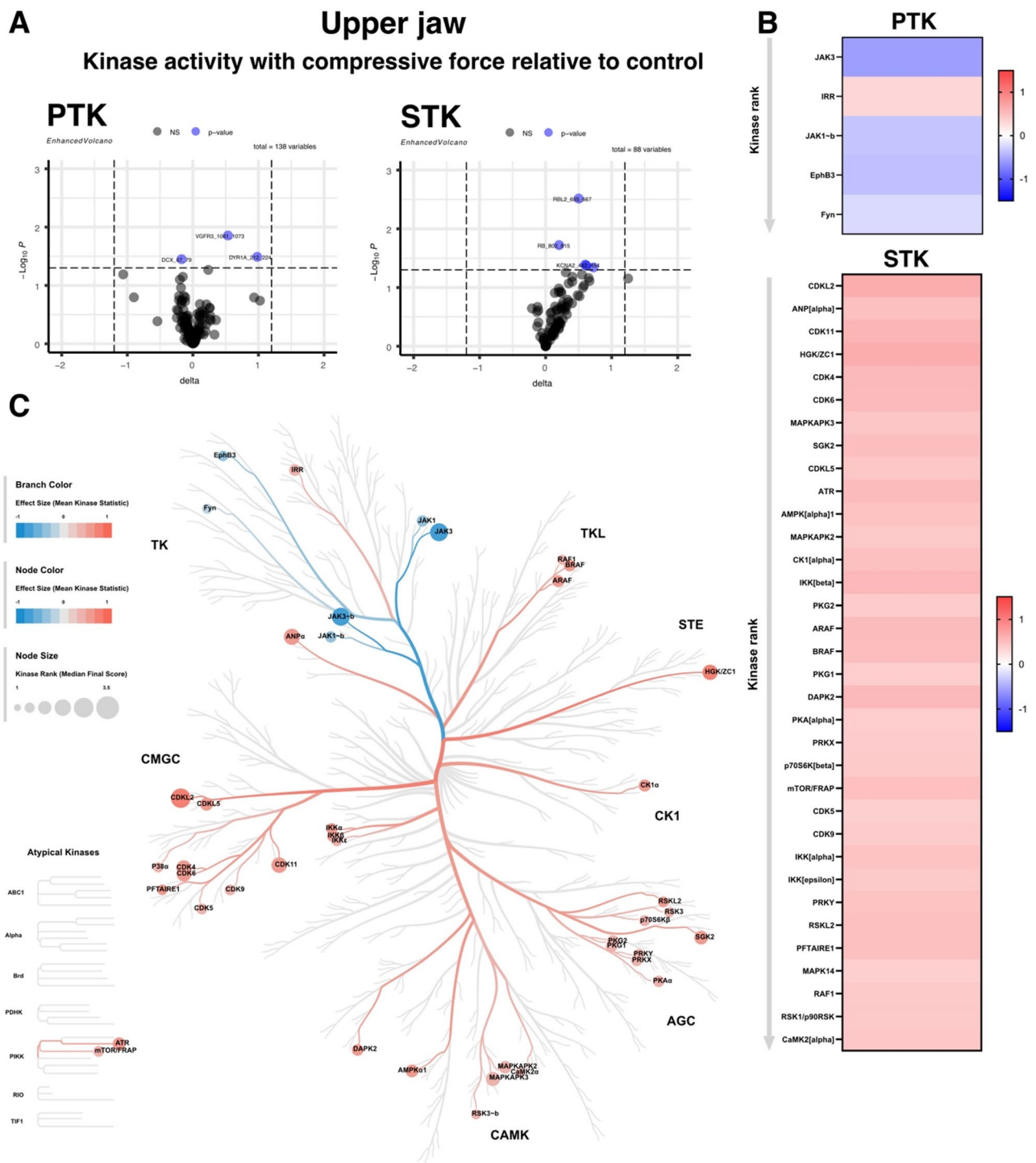


Fig. 3 Compressive force induced a strong up-regulation of PTK phosphorylation in upper jaw. **A** Volcano plots of differentially phosphorylated PTK and STK peptides in arrays exposed to mandibular PDLSC lysates. The x-axis shows the effect size (delta) and the y-axis shows the significance (-Log₁₀ p-value). Blue spots represent peptides whose phosphorylation levels are significantly different between the stimulated and control condition **B** Heatmap of significantly different kinase activity in upper jaw PDLSC, compressive force relative to control, without stimulation of seven donors. The red colour reflects increased activity, while the blue colour reflects decreased activity. **C** Combined PTK and STK kinome tree. Kinase activity is shown on the phylogenetic tree of the human protein kinase family. Dot size indicates specificity score and colour indicates kinase statistic (comparative force vs. control). PTK=phosphotyrosine kinase, STK=serine-threonine kinase. (The data shown are derived from experiments performed with PDLSCs obtained from seven different donors.)

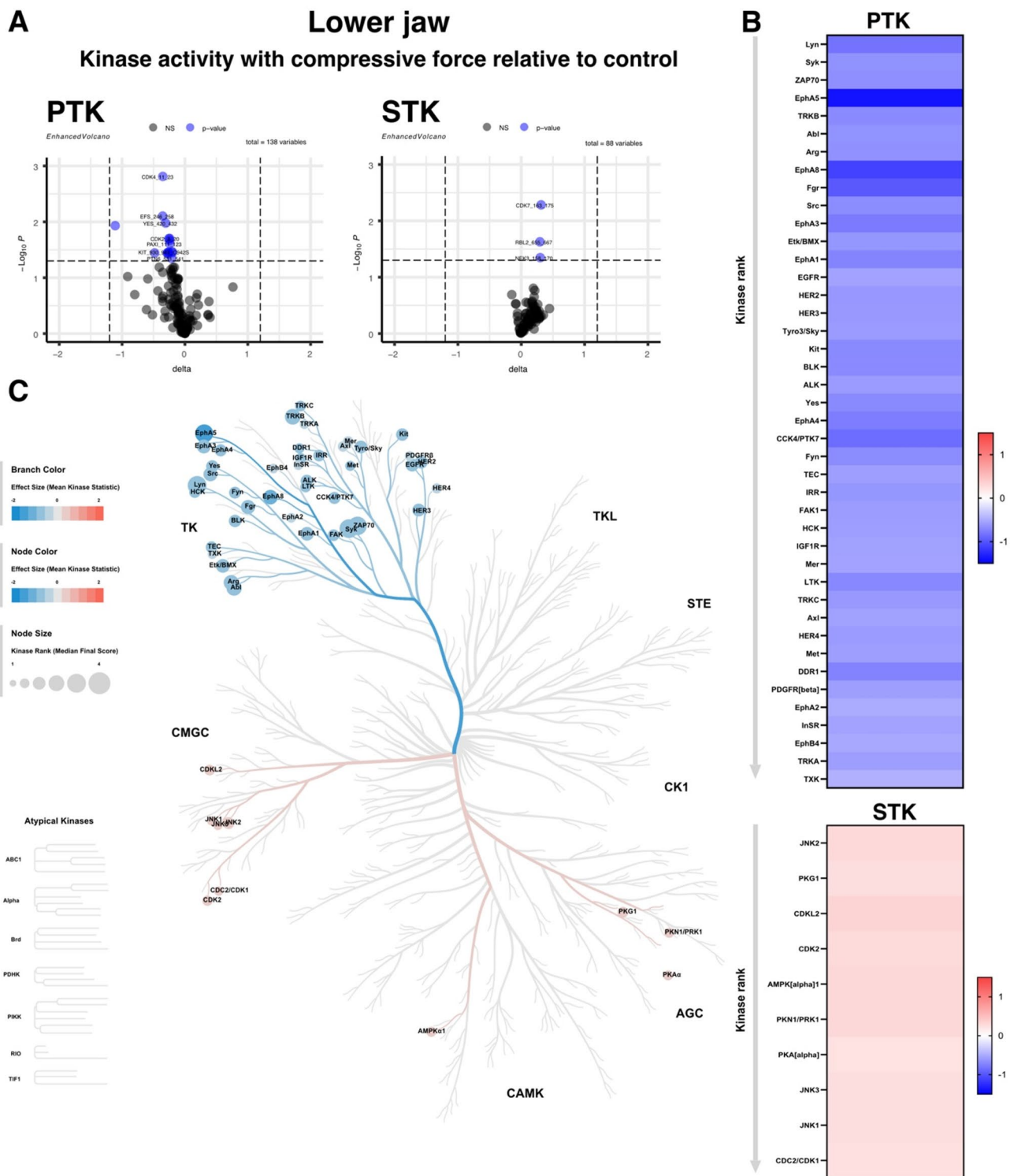


Fig. 4 Compressive force induced a strong downregulation of PTK activity in lower jaw. **A** Volcano plots of differentially phosphorylated PTK and STK phosphosites in arrays exposed to lower jaw PDLSC lysates. The x-axis shows the effect size (delta) and the y-axis shows the significance ($-\log_{10}$ p-value). Blue spots are peptides whose phosphorylation is significantly different between the stimulated and control condition ($p < 0.05$, unpaired t-test). **B** Heatmap of significant differently kinases activity in lower jaw PDLSC, compressive force relative to control. Red colour reflects increased activity, while blue colour reflects decreased activity. **C** Combined PTK and STK kinome tree. Kinase activity is shown on the phylogenetic tree of the human protein kinase family. Dot size indicates specificity score and colour indicates kinase statistic (comparative force vs. control). PTK=phosphotyrosine kinase, STK=serine-threonine kinase. (The data shown are derived from experiments performed with PDLSCs obtained from seven different donors.)

Table 4 Pathway prediction

Regulated only in lower jaw			Regulated in both jaws			Regulated only in upper jaw		
Inflammation								
ID	Description	KinaseRatio	ID	Description	KinaseRatio	ID	Description	KinaseRatio
R-HSA-2,682,334	EPH-Ephrin signaling	12/47	R-HSA-3,928,664	Ephrin signaling	3/47	R-HSA-450,302	activated TAK1 mediates p38 MAPK activation	3/33
R-HSA-450,321	JNK (c-Jun kinases) phosphorylation and activation	3/47	hsa04657	IL-17 signaling pathway	3/44	R-HSA-389,357	CD28 dependent PI3K/Akt signaling	2/33
R-HSA-199,418	Negative regulation of the PI3K/AKT network	10/47	WP286	IL-3 signaling pathway	7/47	GO:0071353	cellular response to interleukin-4	2/39
R-HSA-6,811,558	PI5P, PP2A and IER3 Regulate PI3K/AKT Signaling	10/47	hsa04750	Inflammatory mediator regulation of TRP channels	6/44	GO:0019221	cytokine-mediated signaling pathway	6/39
GO:0043551	regulation of phosphatidylinositol 3-kinase activity	7/52	R-HSA-448,424	Interleukin-17 signaling	3/47	R-HSA-198,753	ERK/MAPK targets	2/33
			R-HSA-450,294	MAP kinase activation	3/47	WP195	IL-1 signaling pathway	4/35
			R-HSA-5,683,057	MAPK family signaling cascades	12/47	WP49	IL-2 signaling pathway	5/35
			WP382	MAPK signaling pathway	8/47	WP395	IL-4 signaling pathway	5/35
			hsa04010	MAPK signaling pathway	16/44	WP127	IL-5 signaling pathway	3/35
			R-HSA-5,684,996	MAPK1/ MAPK3 signaling	11/47	WP205	IL-7 signaling pathway	3/35
			R-HSA-166,166	MyD88-independent TLR4 cascade	3/47	R-HSA-8,983,432	Interleukin-15 signaling	2/33
			WP4172	PI3K-Akt signaling pathway	14/47	R-HSA-451,927	Interleukin-2 family signaling	2/33
			hsa04151	PI3K-Akt signaling pathway	17/44	R-HSA-9,020,558	Interleukin-2 signaling	2/33
			R-HSA-1,257,604	PIP3 activates AKT signaling	10/47	R-HSA-8,854,691	Interleukin-20 family signaling	2/33
			R-HSA-5,673,001	RAF/MAP kinase cascade	10/47	R-HSA-9,020,958	Interleukin-21 signaling	2/33
			R-HSA-449,147	Signaling by Interleukins	10/47	R-HSA-1,266,695	Interleukin-7 signaling	2/33
			R-HSA-187,687	Signalling to ERKs	2/47	hsa04630	JAK-STAT signaling pathway	4/33
			hsa04668	TNF signaling pathway	3/44	R-HSA-5,674,135	MAP2K and MAPK activation	3/33

Table 4 (continued)

Regulated only in lower jaw			Regulated in both jaws			Regulated only in upper jaw		
	R-HSA-168,142	Toll Like Receptor 10 (TLR10) Cascade	3/47		R-HSA-5,684,264	MAP3K8 (TPL2)-dependent MAPK1/3 activation	2/33	
	R-HSA-181,438	Toll Like Receptor 2 (TLR2) Cascade	3/47		WP422	MAPK cascade	4/35	
	R-HSA-168,164	Toll Like Receptor 3 (TLR3) Cascade	3/47		R-HSA-5,675,221	Negative regulation of MAPK pathway	3/33	
	R-HSA-168,176	Toll Like Receptor 5 (TLR5) Cascade	3/47		R-HSA-171,007	p38MAPK events	3/33	
	R-HSA-168,181	Toll Like Receptor 7/8 (TLR7/8) Cascade	3/47		GO:0007259	receptor signaling pathway via JAK-STAT	4/39	
	R-HSA-168,138	Toll Like Receptor 9 (TLR9) Cascade	3/47		GO:0070670	response to interleukin-4	2/39	
	R-HSA-168,179	Toll Like Receptor TLR1:TLR2 Cascade	3/47		WP3851	TLR4 signaling and tolerance	3/35	
	R-HSA-168,188	Toll Like Receptor TLR6:TLR2 Cascade	3/47		R-HSA-75,893	TNF signaling	4/33	
	hsa04620	Toll-like receptor signaling pathway	3/44		R-HSA-166,016	Toll Like Receptor 4 (TLR4) Cascade	7/33	
	R-HSA-937,061	TRIF(TICAM1)-mediated TLR4 signaling	3/47		R-HSA-168,898	Toll-like Receptor Cascades	7/33	
					WP75	Toll-like receptor signaling pathway	4/35	
					WP3858	Toll-like receptor signaling related to MyD88	3/35	
					R-HSA-933,542	TRAF6 mediated NF-kB activation	2/33	
					WP4482	Vitamin D in inflammatory diseases	3/35	
Bone remodeling								
GO:0098751	bone cell development	2/52	WP673	ErbB signaling pathway	11/47	R-HSA-3,858,494	Beta-catenin independent WNT signaling	3/33
GO:0198738	cell-cell signaling by wnt	5/52	hsa04012	ErbB signaling pathway	11/44	WP1434	Osteopontin signaling	2/35

Table 4 (continued)

Regulated only in lower jaw			Regulated in both jaws			Regulated only in upper jaw		
GO:0001503	ossification	5/52	hsa04380	Osteoclast differentiation	6/44	R-HSA-195,721	Signaling by WNT	4/33
GO:0033687	osteoblast proliferation	2/52	WP2018	RANKL/RANK signaling pathway	6/47	WP363	Wnt signaling pathway	3/35
GO:0030177	positive regulation of Wnt signaling pathway	4/52	hsa04310	Wnt signaling pathway	4/44			
GO:0046850	regulation of bone remodeling	2/52						
GO:0045124	regulation of bone resorption	2/52						
R-HSA-8,941,326	RUNX2 regulates bone development	3/47						
R-HSA-8,940,973	RUNX2 regulates osteoblast differentiation	3/47						
R-HSA-1,227,986	Signaling by ERBB2	7/47						
Mechanical/external Stimulation								
GO:0042490	mechano-receptor differentiation	2/52	GO:0032103	positive regulation of response to external stimulus	11/52			
WP4534	Mechanoregulation and pathology of YAP/TAZ	4/47						
GO:0050954	sensory perception of mechanical stimulus	3/52						
Vascularisation								
hsa04015	Rap1 signaling pathway	8/44	R-HSA-194,138	Signaling by VEGF	5/47	hsa04370	VEGF signaling pathway	4/33
			R-HSA-4,420,097	VEGFA-VEGFR2 Pathway	5/47			
			WP3888	VEGFA-VEGFR2 signaling pathway	10/47			

Selected predicted pathways from the databases GO (GO:), KEGG (hsa), Wikipathways (WP) and enriched pathways (R-HAS) with relevance for the biological processes of periodontal remodeling

were downregulated and many STKs were upregulated in the upper jaw, the opposite was true in the lower jaw, with many downregulated PTKs and few upregulated STKs. Interestingly, only some of the affected kinases were equally regulated in the maxilla and mandible. IRR was upregulated in the maxilla and downregulated in the mandible, while Fyn was downregulated in both jaws. The STKs (CDKL2, AMPK[alpha]1, PKG1, and PKA[alpha]) were upregulated in both jaws. All other regulated PTKs

and STKs were regulated explicitly in only one jaw. This suggests that, under mechanical stress, only a minority of regulated kinases exhibit a common signalling pathway, while the majority of kinases indicate jaw-specific pathways.

Insulin receptor-related receptor (IRR) is the only kinase that is regulated inversely in both jaws, and first undergoes autophosphorylation. This modification activates its intrinsic tyrosine kinase domain, which in turn

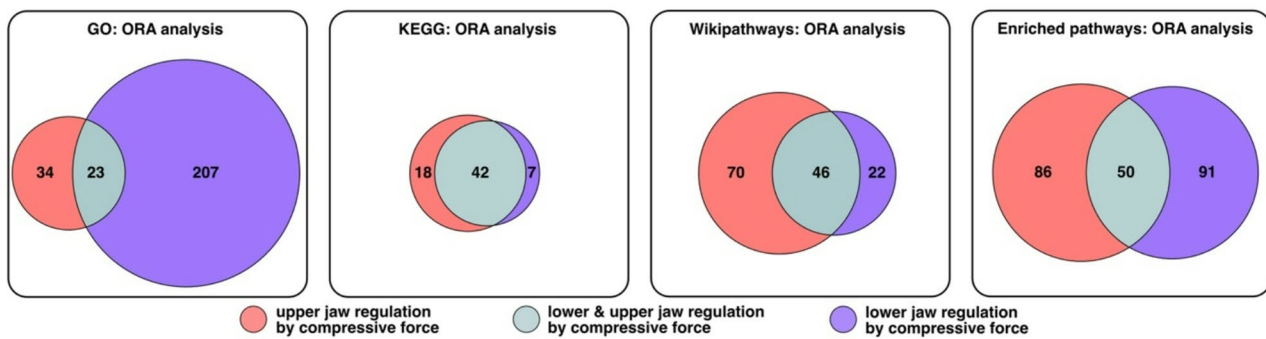


Fig. 5 Overrepresentation analysis (ORA)

triggers the phosphorylation of downstream intracellular targets. By this, IRR facilitates the initiation of two important cellular signaling pathways: the PI3K-AKT axis and the MAPK cascade, both of which are essential for mediating metabolic and growth responses. The activation of IRR by mechanical stimulation is not yet fully understood [39–41]. Fyn, the second PTK which is regulated in both jaws, is known to be involved in regulating cell adhesion, migration, and cytoskeletal dynamics through integrin, FAK, and PI3K/AKT and MAPK signaling [42]. The commonality between Fyn and IRR, a connection to the PI3k-AKT axis and MAPK cascade, suggests they play a relevant role in the cellular response to mechanical stress during orthodontic tooth movement, as it is known that these signalling pathways are regulated under this condition. The same applies to the four STKs regulated in both jaws.

Based on the differences in kinase activity, possible signaling pathways modulated by the mechanical stimulus were reconstructed using the GO, KEGG, Wikipathways, and Enriched Pathways databases. Our analyses revealed distinct relevant signaling pathways for the upper and lower jaws. Interestingly, in addition to numerous signaling pathways that had not previously been associated with mechanical stimulation, the analyses also identified signalling pathways such as PI3K-AKT, MAPK and Wnt, whose relevance for periodontal remodelling had already been demonstrated [5, 9].

In summary, our findings validate the hypothesis that PDLSCs from the maxilla and mandible exhibit distinct intrinsic properties, reflected in divergent kinase activity profiles in response to mechanical stimulation. These molecular differences likely contribute to clinically observed variations in tooth movement dynamics and alveolar remodeling capacity. The identification of region-specific kinases provides a valuable entry point for future mechanistic studies and may inform the development of targeted, site-specific therapeutic strategies in orthodontics and periodontal regeneration.

Conclusion

PDLSCs derived from the upper and lower jaw exhibit distinct intrinsic properties, reflected in differential activation of kinase-driven regulatory pathways under static mechanical stimulation. Recognizing and incorporating these jaw-specific molecular signatures in future research may enhance our understanding of regionally tailored signaling mechanisms, ultimately contributing to more precise approaches for the management of orthodontic tooth movement and periodontal wound healing.

Supplementary Information

The online version contains supplementary material available at <https://doi.org/10.1186/s13287-025-04778-5>.

Supplementary Material 1

Supplementary Material 2

Acknowledgements

This project was supported by the Clinician Scientist Program of the Faculty of Medicine of the RWTH Aachen University (to C.N.). The authors declare that they have not use AI-generated work in this manuscript.

Author contributions

Conceptualization, C.N., M.W. and R.B.C.; methodology, C.N., R.B.C.; supervision, R.B.C. and M.W.; project administration, C.N. and R.B.C.; data acquisition, C.N.; R.B.C., S.L.M. and E.P.C.v.d.V.; data analysis, C.N.; R.B.C., S.L.M. and E.P.C.v.d.V.; data interpretation, C.N.; R.B.C., S.L.M., L.J.S., F.H., Y.S. and E.P.C.v.d.V.; writing - original draft preparation, C.N.; writing - review and editing, R.B.C., C.N.; M.W., S.L.M., L.J.S., F.H., Y.S. and E.P.C.v.d.V.; visualization, C.N., E.P.C.v.d.V., S.L.M. and R.B.C.; funding acquisition, E.P.C.v.d.V., M.W., R.B.C. All authors have read and agreed to the published version of the manuscript.

Funding

Open Access funding enabled and organized by Projekt DEAL. M.W. and R.B.C. were supported by the Deutsche Forschungsgemeinschaft (DFG, German Research Foundation), Project-ID 504777725, Project-ID 490932300 and Project-ID 559483338. This work was also supported by the Corona Foundation (S199/10084/2021), and by the Deutsche Forschungsgemeinschaft (DFG) (SFB TRR219 – Project-ID 322900939; subproject M07) to E.P.C.v.d.V.

Data availability

The datasets supporting the conclusions of this article are included within the article and its additional files.

Declarations

Ethics approval and consent to participate

The collection and use of periodontal cells derived from discarded patient biomaterial was authorized by the Ethics Committee of the University of Aachen, Germany (approval number EK 374/19), under the title (translated) "Isolation and characterization of cells from human periodontium", granted on November 19, 2019.

Competing interests

The authors declare no competing interests.

Author details

¹Department of Orthodontics, University Hospital RWTH Aachen, Pauwelsstraße 30, 52074 Aachen, Germany

²Department of Internal Medicine I, Aachen-Maastricht Institute for Cardio-Renal Disease (AMICARE), Institute for Molecular Cardiovascular Research (IMCAR), University Hospital Aachen, RWTH Aachen University, Aachen, Germany

³Institute for Cardiovascular Prevention (IPEK), Ludwig-Maximilians-Universität, Munich, Germany

⁴Department of Biochemistry, CARIM, Maastricht University, Maastricht, The Netherlands

⁵Institute of Experimental Medicine and Systems Biology, RWTH Aachen University, Aachen, Germany

⁶Department of Polymer Therapeutics, Institute for Experimental Molecular Imaging, RWTH Aachen University Clinic, Aachen, Germany

⁷Department of Oral and Maxillofacial Surgery, University Hospital RWTH Aachen, Pauwelsstraße 30, 52074 Aachen, Germany

Received: 4 August 2025 / Accepted: 22 October 2025

Published online: 07 November 2025

References

1. Aveic S, Craveiro RB, Wolf M, Fischer H. Current trends in in vitro modeling to mimic cellular crosstalk in periodontal tissue. *Adv Healthc Mater.* 2021;10:2001269. <https://doi.org/10.1002/ADHM.202001269>.
2. de Jong T, Bakker AD, Everts V, Smit TH. The intricate anatomy of the periodontal ligament and its development: lessons for periodontal regeneration. *J Periodontol Res.* 2017;52:965–74. <https://doi.org/10.1111/JRE.12477>.
3. Meng X, Zhu Y, Tan H, Daraqel B, Ming Y, Li X, et al. The cytoskeleton dynamics-dependent LINC complex in periodontal ligament stem cells transmits mechanical stress to the nuclear envelope and promotes YAP nuclear translocation. *Stem Cell Res Therapy.* 2024;15:1–19. <https://doi.org/10.1186/S13287-024-03884-0/FIGURES/7>.
4. Li Y, Li Y, Liu C, Yu X, Gan Z, Xiang L, et al. Mechanical force-activated CD109 on periodontal ligament stem cells governs osteogenesis and osteoclast to promote alveolar bone remodeling. *Stem Cells Transl Med.* 2024;13:812–25. <https://doi.org/10.1093/STCLTM/SZAE035>.
5. Roth CE, Craveiro RB, Niederau C, Malyaran H, Neuss S, Jankowski J, et al. Mechanical compression by simulating orthodontic tooth movement in an in vitro model modulates phosphorylation of AKT and MAPKs via TLR4 in human periodontal ligament cells. *Int J Mol Sci.* 2022. <https://doi.org/10.3390/IJMS23158062>.
6. Malyaran H, Radermacher C, Craveiro RB, Kühnel MP, Jonigk D, Wolf M, et al. Angiogenic potential in periodontal stem cells from upper and lower jaw: A pilot study. *J Periodontol.* 2024;95:662–72. <https://doi.org/10.1002/JPER.24-0070>.
7. Burstone CJ. The biomechanics of tooth movement. *Vistas in orthodontics.* Philadelphia: Lea & Febiger; 1962. pp. 197–213.
8. Krishnan V, Davidovitch Z. Cellular, molecular, and tissue-level reactions to orthodontic force. *Am J Orthod Dentofac Orthop.* 2006;129:469.e1–469.e32. <https://doi.org/10.1016/j.jado.2005.10.007>.
9. Li Y, Zhan Q, Bao M, Yi J, Li Y. Biomechanical and biological responses of periodontium in orthodontic tooth movement: up-date in a new decade. *Int J Oral Sci.* 2021;13. <https://doi.org/10.1038/S41368-021-00125-5>.
10. Wen X, Pei F, Jin Y, Zhao Z. Exploring the mechanical and biological interplay in the periodontal ligament. *Int J Oral Sci.* 2025;17:1. <https://doi.org/10.1038/s41368-025-00354-y>.
11. Davidovitch Z, Krishnan V. Role of basic biological sciences in clinical orthodontics: a case series. *Am J Orthod Dentofac Orthop.* 2009;135:222–31. <https://doi.org/10.1016/j.jado.2007.03.028>.
12. D'Apuzzo F, Cappabianca S, Ciavarella D, Monsurrò A, Silvestrini-Biavati A, Perillo L. Biomarkers of periodontal tissue remodeling during orthodontic tooth movement in mice and men: overview and clinical relevance. *Sci World J.* 2013;2013. <https://doi.org/10.1155/2013/105873>.
13. Omi M, Mishina Y. Roles of osteoclasts in alveolar bone remodeling. *Genesis.* 2022;60:e23490. <https://doi.org/10.1002/DVG.23490>.
14. Giannopoulou C, Dudic A, Pandis N, Kiliaridis S. Slow and fast orthodontic tooth movement: an experimental study on humans. *Eur J Orthod.* 2016;38:404–8. <https://doi.org/10.1093/EJO/CJV070>.
15. Navya S, Prashantha GS, Sabrish S, Roshan MS, Mathew S. Evaluation of the effect of local administration of PRP vs vitamin D3 on the rate of orthodontic tooth movement and the associated external apical root resorption. *J Oral Biol Craniofac Res.* 2022;12:879–84. <https://doi.org/10.1016/JJOBRCR.2022.09.011>.
16. Deguchi T, Takano-Yamamoto T, Yabuuchi T, Ando R, Roberts WE, Garetto LP. Histomorphometric evaluation of alveolar bone turnover between the maxilla and the mandible during experimental tooth movement in dogs. *Am J Orthod Dentofac Orthop.* 2008;133:889–97. <https://doi.org/10.1016/j.jado.2006.12.013>.
17. Chugh T, Ganeshkar SV, Revankar AV, Jain AK. Quantitative assessment of interradicular bone density in the maxilla and mandible: implications in clinical orthodontics. *Prog Orthod.* 2013;14:1–8. <https://doi.org/10.1186/2196-1042-14-38/TABLES/4>.
18. Devlin H, Horner K, Ledgerton D. A comparison of maxillary and mandibular bone mineral densities. *J Prosthet Dent.* 1998;79:323–7. [https://doi.org/10.1016/S0022-3913\(98\)70245-8](https://doi.org/10.1016/S0022-3913(98)70245-8).
19. Chugh T, Jain AK, Jaiswal RK, Mehrotra P, Mehrotra R. Bone density and its importance in orthodontics. *J Oral Biol Craniofac Res.* 2013;3:92–7. <https://doi.org/10.1016/JJOBRCR.2013.01.001>.
20. Wu V, Schulten EAJM, Helder MN, ten Bruggenkate CM, Bravenboer N, Klein-Nulend J. Bone vitality and vascularization of mandibular and maxillary bone grafts in maxillary sinus floor elevation: A retrospective cohort study. *Clin Implant Dent Relat Res.* 2023;25:141–51. <https://doi.org/10.1111/CID.13142>.
21. Brennisse CV, Squier CA. Blood flow in maxilla and mandible of normal and atherosclerotic rhesus monkeys. *J Oral Pathol Med.* 1985;14:800–8. <https://doi.org/10.1111/J.1600-0714.1985.TB00470.X>.
22. Radermacher C, Craveiro RB, Jahnhen-Dechent W, Beier JP, Bülow A, Wolf M, et al. Impact of compression forces on different mesenchymal stem cell types regarding orthodontic indication. *Stem Cells Transl Med.* 2024;13:1028. <https://doi.org/10.1093/STCLTM/SZAE057>.
23. Tou GADA, Diniz IMA, Ferreira MVL, Mesquita RA, Yamauti M, Silva TA, et al. Evaluation of periodontal parameters and gingival crevicular fluid cytokines in children with anterior open bite receiving passive orthodontic treatment with a spur. *Korean J Orthod.* 2022;52:142–9. <https://doi.org/10.4041/KJOD.2022.52.2.142>.
24. Mert S, Malyaran H, Craveiro RB, Wolf M, Modabber A, Jahnhen-Dechent W, et al. Comparative analysis of proliferative and multilineage differentiation potential of human periodontal ligament stem cells from maxillary and mandibular molars. *J Periodontol.* 2023;94:882–95. <https://doi.org/10.1002/JPER.22-0706>.
25. Malyaran H, Craveiro RB, Mert S, Niederau C, Maas SL, van der Vorst EPC, et al. Identifying differences in molecular characteristics relevant for remodeling of periodontal ligament stem cells from the upper and lower jaw. *Int J Mol Sci.* 2024;25. <https://doi.org/10.3390/IJMS25063207>.
26. Kanzaki H, Chiba M, Shimizu Y, Mitani H. Periodontal ligament cells under mechanical stress induce osteoclastogenesis by receptor activator of nuclear factor κB ligand Up-Regulation via prostaglandin E2 synthesis. *J Bone Miner Res.* 2002;17:210–20. <https://doi.org/10.1359/jbmr.2002.17.2.210>.
27. Blighe KRSLM, EnhancedVolcano. Publication-ready volcano plots with enhanced colouring and labeling. 2025.
28. Wu T, Hu E, Xu S, Chen M, Guo P, Dai Z, et al. ClusterProfiler 4.0: A universal enrichment tool for interpreting omics data. *Innov (Cambridge (Mass)).* 2021;2. <https://doi.org/10.1016/J.XINN.2021.100141>.
29. Wickham H. ggplot2: elegant graphics for data analysis. New York: Springer; 2016.
30. Yu G, Wang LG, Yan GR, He QY. DOSE: an R/Bioconductor package for disease ontology semantic and enrichment analysis. *Bioinformatics.* 2015;31:608–9. <https://doi.org/10.1093/BIOINFORMATICS/BTU684>.

31. Yu G, He QY. ReactomePA: an R/Bioconductor package for reactome pathway analysis and visualization. *Mol Biosyst.* 2016;12:477–9. <https://doi.org/10.1039/C5MB00663E>.
32. Erdfelder E, Faul F, Buchner A. GPOWER: A general power analysis program. *Behavior research methods. Instruments Computers.* 1996;28:1–11. <https://doi.org/10.3758/BF03203630/METRICS>.
33. Dominici M, Le Blanc K, Mueller I, Slaper-Cortenbach I, Marini FC, Krause DS, et al. Minimal criteria for defining multipotent mesenchymal stromal cells. The international society for cellular therapy position statement. *Cytotherapy.* 2006;8:315–7. <https://doi.org/10.1080/14653240600855905>.
34. Iwayama T, Sakashita H, Takedachi M, Murakami S. Periodontal tissue stem cells and mesenchymal stem cells in the periodontal ligament. *Japanese Dent Sci Rev.* 2022;58:172–8. <https://doi.org/10.1016/J.JDSR.2022.04.001>.
35. Niederau C, Bhargava S, Schneider-Kramman R, Jankowski J, Craveiro RB, Wolf M. Xanthohumol exerts anti-inflammatory effects in an in vitro model of mechanically stimulated cementoblasts. *Sci Rep J.* 2022;12:14970. <https://doi.org/10.1038/s41598-022-19220-6>.
36. Ullrich N, Schröder A, Jantsch J, Spanier G, Proff P, Kirschneck C. The role of mechanotransduction versus hypoxia during simulated orthodontic compressive strain—an in vitro study of human periodontal ligament fibroblasts. *Int J Oral Sci.* 2019;11:1–10. <https://doi.org/10.1038/s41368-019-0066-x>.
37. Weider M, Schröder A, Docheva D, Rodrian G, Enderle I, Seidel CL, et al. A human periodontal ligament fibroblast cell line as a new model to study periodontal stress. *Int J Mol Sci.* 2020;21:1–10. <https://doi.org/10.3390/ijms21217961>.
38. Janjic M, Docheva D, Trickovic Janjic O, Wichelhaus A, Baumert U. In vitro Weight-Loaded cell models for Understanding mechanodependent molecular pathways involved in orthodontic tooth movement: A systematic review. *Stem Cells Int* 2018. <https://doi.org/10.1155/2018/3208285>.
39. Yunn NO, Kim J, Ryu SH, Cho Y. A Stepwise activation model for the insulin receptor. *Experimental Mol Med* 2023. 2023;55:10. <https://doi.org/10.1038/s12276-023-01101-1>.
40. Gehart H, Kumpf S, Ittner A, Ricci R. MAPK signalling in cellular metabolism: stress or wellness? *EMBO Rep.* 2010;11:834–40. <https://doi.org/10.1038/EMBO.R.2010.160>.
41. White MF, Kahn CR. Insulin action at a molecular level – 100 years of progress. *Mol Metab.* 2021;52. <https://doi.org/10.1016/J.MOLMET.2021.101304>.
42. Peng SF, Fu Y. FYN: emerging biological roles and potential therapeutic targets in cancer. *J Transl Med.* 2023;21. <https://doi.org/10.1186/S12967-023-03930-0>.

Publisher's note

Springer Nature remains neutral with regard to jurisdictional claims in published maps and institutional affiliations.